Defence Technology 17 (2021) 305–314

Contents lists available at ScienceDirect

Defence Technology

journal homepage: www.keaipublishing.com/en/journals/defence-technology

Ricochet quantification using a multiple sensor approach☆

Michael Muster*, Amer Hameed, David Wood

Centre for Defence Engineering, Cranfield University, Defence Academy of the United Kingdom, Shrivenham, SN6 8LA, UK

ARTICLE INFO

Article history:
Received 9 December 2019
Received in revised form
22 January 2020
Accepted 17 February 2020
Available online 20 February 2020

Keywords:
Ricochet analysis
Small-calibre ammunition
Velocity measurement
Thermography

ABSTRACT

This study investigates the ricochet behaviour of three different small-arms projectile types using a novel ricochet measuring device. The results can be used to estimate the danger potential of ricochets on shooting ranges.A ricochet is the change of direction and velocity of a projectile after impacting an oblique surface. This impact produces strong vibrations on a rigid plate.

During this impact, flexural waves travel radially outwards from the point of impact. These waves are used to determine the properties of the impactor with accelerometers situated on the target surface. With the use of two measurement plates, one can produce a ricochet and detect the velocity at the same time.

Accelerometers are suitable for accurate momentum measurements of single impacts. However, depending upon strike velocity and the impact angle, a ricochet can separate in multiple fragments after being deflected. From the operational safety perspective, these fragments need to be detected, as well. The approach of a coupled sensor concept was chosen to solve this problem.

Thermographic sensors were additionally used to visualise the heat which is produced after penetrating a rubber layer pasted in front of the steel target plate. With this approach one was able to detect the position of impact. The investigations showed that the measurement system performance is better with a multiple sensor design, which includes accelerometers for the velocity, impact strength and partly the position measurement, while the thermographic sensor was used for the position measurement and partly the momentum measurement.

The investigated ammunition showed plausible fragmentation behaviour, and the results can already be used to estimate the danger potential of different ammunition types. Frangible projectiles fragment to small particles already after being deflected under a small angle. However, Full Metal Jacket projectiles with or without a steel core do not fragment under angles which are less than 5°.

The objective of the paper is to demonstrate the possibility of measuring the complex ricochet mechanics of small projectiles using standard accelerometers with the adequate signal processing approach. This measuring system is supported by an off the shelf thermographic camera.

1. Introduction

The aim of this work is to investigate the performance of a novel measurement device capable of measuring ricochets of small-calibre ammunition. Small arms are extensively used during manoeuvre-based operations.

Any high-speed fragment ricocheting from fragmenting projectiles is a safety hazard for personnel operating in the vicinity. It is essential, therefore, to evaluate the potential danger zone of ricocheting particles generated by projectiles.

Small-calibre projectiles are objects that weigh from 2 to 10 g, which travel at supersonic speed and produce strong acceleration signals on impacting an object such as witness plate which are used for ballistic investigations. Due to their high speed and rotation rates, projectiles are generally challenging to characterise during flight and impact, even with high-frequency sensors.

Sensors mounted on small arms projectiles, for ballistic tests, would be too bulky and affect the flight path. Ricochet characterisation is necessary for important applications like the estimation of

☆ Cranfield Defence and Security, Cranfield University, Shrivenham, Swindon SN6 8LA, United Kingdom.

* Corresponding author.
E-mail addresses: michael.muster@cranfield.ac.uk (M. Muster), a.hameed@cranfield.ac.uk (A. Hameed), d.wood@cranfield.ac.uk (D. Wood).

Peer review under responsibility of China Ordnance Society

https://doi.org/10.1016/j.dt.2020.02.017
2214-9147/

range danger areas of shooting ranges. For the desired applications, one needs to know the position of impact and the momentum transmitted into the plate. To be known are also the time and distance between the first and second impact, where the ricochets are finally stopped. Using this information, one can measure the residual energy, fragment weight and deflection angle of the projectile after impact, as well as the velocity.

The velocity can be derived easily by using a Time of Flight (TOF) approach with two trigger devices. In the proposed system, the two sensor plates are considered as trigger devices. However, the procedure is similar to the well-known trigger-foil system, which is often used to trigger ballistic events such as e.g. ballistic events in high-speed imaging [1] or general investigations like multiple impacts [2]. The idea behind foil triggers is that two electrically conductive foils (preferably of aluminium) are set up directly behind each other. During the penetration process, a short circuit is generated which can be used as a trigger. Using two of these trigger devices and with the known distance between them, one can calculate the velocity by applying the TOF. This approach is shown by Yan et al. [3].

The triggering system in the case proposed here relies on wave propagation in the plate material. The idea is similar to the acoustical approach described in the notes of Michael Courtney [4]. He investigated the time of flight with a high-resolution microphone and placed this microphone equidistant between the target and the barrel muzzle. With the known distance between target and barrel muzzle, plus the time difference of the two acoustic signals, one could recalculate the mean velocity of the projectile. The acoustic signals come from the muzzle burst and the impact sound burst when the projectile hits the target (in this case a steel plate). The main challenge for in detail impact quantification on steel plates has to do with enormous decelerations and big deformations in a short time. This is why sensors mounted on witness plates, in the proposed case of steel, are widely used for impact detection.

Impact detection units with plates rely on e.g. Impact Soft-Recovery Experiments [5]. In this case, the target under investigation is a brittle plate, monitored by an interferometer. The projectile's impact generates strong vibrations, which can be used to characterise the nature of the impact. Espinosa et al. [6] revealed that it is possible to get a cleaner raw signal from the target plate by using a star-shaped geometry. Their tests showed that one can significantly minimise the effect of the outer layer of the plate on the impact zone itself. Like interferometers, accelerometers are frequently used to determine properties of the impact such as the impact position or the momentum [7–9]. One of the major sources of measurement inaccuracies are random and reflected vibrations [10]. Hammetter et al. used an array of accelerometers fixed on the plate to determine the momentum transferred. He showed that geometrical properties of the detecting plate itself might lead to inaccurate measurements.

Another source of measurement inaccuracy is electronic filtering of the acceleration data. As a best practice for shock investigations, accelerometers are mechanically insulated [11]. Severe mechanical shocks such as bullet impact typically lead to six degrees of freedom accelerations represented in broadband frequencies. These frequencies make it difficult to determine the overall momentum [6] or the position. Mechanical insulators combined with electrical filters were found to be an appropriate way to overcome this problem.

The impacting body excites the witness plate within a very short time in a non-linear and random vibration regime, where scattering and reflections of vibrations at boundaries will occur [12,13]. Right after the impact is the moment where the point of interest occurs, this moment is called the Arrival Time (AT). The AT is defined as the time when the sensor detects the first set of waves, which originates from the impact position.

Consequently, knowing the accurate AT is necessary to recalculate the exact impact position with the Time Difference of Arrival (TDOA) algorithms [14]. TDOA algorithms are nowadays often used and optimised for passive tracking of wireless communication systems [15]. However, the underlying computations for wireless devices tracking and the impact location are the same. The main issue for an accurate triangulation of impact remains accurate AT detection. For flexural group waves travelling in steel at a speed of over 2500 m/s, even minor time errors lead to significant positioning errors. Knowing the speed of sound in the target material and the AT difference are necessary for positioning. Furthermore, by knowing the sensor positions, one can calculate the location of the impact/of the origin of the waves by numerical approaches [16].

Mingzhou et al. showed the possibility of precisely detecting the AT of flexural waves using accelerometers after the impact of a dropped test weight on a large steel plate. This investigation was done in noisy environments like power plants [17]. They used a sophisticated decomposition algorithm combined with the Hilbert Huang Transformation. They found that the proposed algorithm was capable of detecting the AT with a precision of several milliseconds. The main reason for the inaccuracies was still the noise in the signal. In an idealised case, to lower the noise, flexural and compression waves emitted from the origin of impact would not be reflected.

The minimization of the reflections can be realised by two approaches: using a plate significantly larger compared with the investigated area (this approach is presented in Ref. [13]), or using a special damping plate. Unique damping plates are needed for both measurement types, momentum measurement and positioning.

An interesting approach is a plate of unique shape with decreasing thickness at the edge (called a wedge shape) in a power-law profile [18]. The different waveforms are eliminated due to internal refraction. However, the power-law shape is challenging to manufacture, which is why it is not used in practical vibration dampers [19].

Possible approaches to manufacture this wedge shape are 3D milling or casting [20], which are cost-intensive. Where hardened steel and supersonic impacts are concerned, such delicate and large structures are unsuitable for ballistic applications. For impact analysis, shapes for more robust structures are desirable.

For hardened steel wear plates suitable to resist supersonic impacts, 2D shapes should be used. Waterjet cutting or plasma cutting could produce such plate designs. Possible shapes that can be manufactured easily are any polygons or any round but two-dimensional shapes.

Star-shaped (polygonal) flyer plates are also able to trap compression waves, as used for standard impact soft-recovery experiments [6]. In the star-shaped plate, much lower-level reflection is observed during impact, which enhances the quality of the raw data in ballistic tests. The edge morphology is capable of serving as a trap for waves and was investigated computationally in Ref. [21].

A combination of star-shaped damping plate, enhanced by using an acoustic black-hole shape for ballistic investigations, is proposed by Muster et al. [22]. A witness and ricochet plate like this are capable of measuring the momentum of an impact accurately.

For more accurate projectile impact position investigations, especially for multiple impacts, it makes sense to search for a different solution. Manrad and Doty [23] describe in their patent an application which captures an impact on an elastic screen which heats up during the penetration process of the projectile. The idea of the patent is to calculate the exact impact coordinates of a single impact. Using this information, it is possible to get a real-time signal out of the computations, which the operator may apply

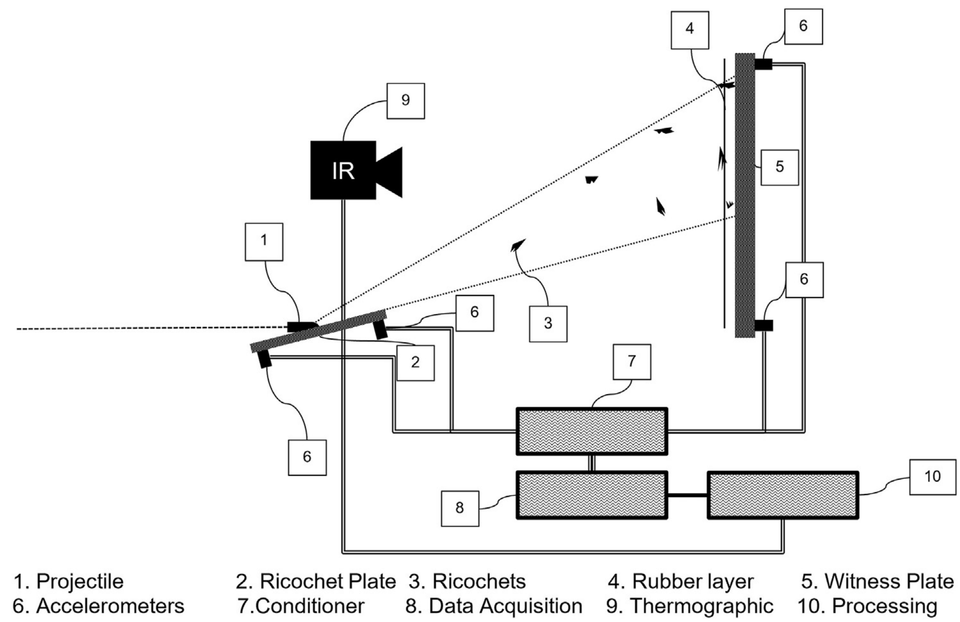

Fig. 1. System layout: under an incident trajectory, the projectile (1) impacts the ricochet plate (2) and gets fragmented and deflected under a certain angle. The deflected fragments (3) fly in the direction of the rubber layer (4) and penetrate it. After penetration, the fragments get stopped on the witness plate (5) which is, like the ricochet plate, equipped with four accelerometers (6). The raw signal of the accelerometers is first conditioned (7) so that it can be digitalised by the Data Acquisition Device (8). The rubber layer, heated up during the penetration process, is observed under thermographic (9) to determine the point of impact with the help of the raw signal of the accelerometers. All signals are processed in the processing unit (10).

during the most realistic possible training. The information about heating up is used to calculate the virtual trajectory of the projectile, not to make any statement about the impact. The process of heating up and the amount of energy transmitted into the screen are not of interest. However, it shows the basic idea and the performance of such thermographic systems.

Thermography in ballistics is also often used to investigate failure mechanisms in composite structures [24–26]. The reason for using high-speed thermography is that different materials of the composite structure are heated for a short time during the penetration process, and this can affect the matrix material, which is often thermoplastic or epoxy resin. These thermal differences are only of short duration and need to be investigated by high-speed thermography.

However, thermography has also its benefits for the investigation of materials like ballistic composite structures, without need for frame rates over 30 per second. Gopalakrishnan et al. [27] showed that it is possible to investigate the damage point of impact on a ballistic sheet impacted by a medium-velocity body using a 50 Hz camera. The studied material with fibres acts more like a monolithic material, as can be seen in the picture taken after several milliseconds.

Another interesting approach to investigate materials using low frame-rate thermography is shown by Duan et al. [28]. They described a system, which assesses the material after damage. They took a general heat source and heated the specimen. This heating-up process was filmed with a low-framerate thermal camera. The outcome was that, with this low-cost approach, it was possible to investigate the failure in the specimen itself accurately. The accuracy was better compared to the state-of-the-art ultrasonic transmission assessment. Soonkyu et al. [29] described a way to inspect wind turbine blades with the use of a laser and thermography. Fractures on large blades are assessed by laser preheating. In case, the damage is allocated to the surface, the specific heat capacity changes. The blade with the damaged zone heats up faster. With such a system, the defect can be precisely detected and investigated.

The sought sensor system is a combination of Gopalakrishnan with the low-framerate thermography of impacts, and the reversed approach of Soonkyu et al. During the penetration of a rubber layer, an impacting projectile dissipates its kinetic energy in lower form by producing heat. This heat is stored so that it can be seen for several seconds after impact.

To increase the positioning accuracy of multiple impacts, a thermographic sensor is used additionally. With this combination, a measurement device can be realised which is capable of working with all kinds of projectiles and quantifying their ricochets. To get a broader picture of the accelerometer measurements, a second sensor type is used a so-called piezoelectric strain gauge. Thanks to their broadband signal acquisition capabilities, these sensor types can identify the condition of large structures [30].

This paper describes a sensor method for ballistic analysis using two plates equipped with four acceleration sensors and a thermographic sensor in combination with a witness rubber layer. The momentum measurement of the projectile or its ricochets is made with specially shaped plates equipped with accelerometers capable of measuring uniaxial accelerations. They are placed in the normal position relative to the plate, which means that only flexural waves will be measured.

2. Material and methods

The ricochet measurement device consists of two main parts. The schematic idea of the system is described in Fig. 1.

First, a heavy ricochet table, see Fig. 2a and b, attached to a pushcart with reliable brakes to ensure that it does not move during impact. The table can be adjusted in height and angle. The ricochet plate is equipped with accelerometers to localise the point where the projectile touches the plate for the first time, and deflects the projectile depending on the angle of the plate.

Second, a heavy metal frame, see Fig. 2c and d, equipped with a second sensor plate at the back, called witness plate. The witness

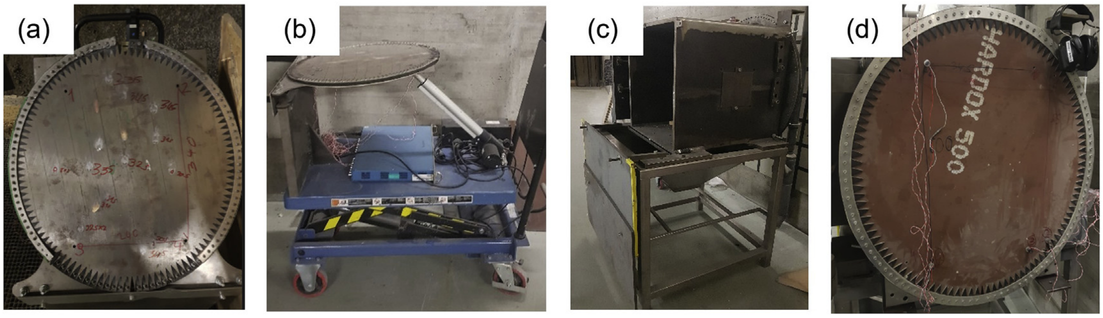

Fig. 2. a–d: Picture (a) shows the ricochet plate, the spikes of the plate are damping structures which allow a better AT detection, which is important for the precise triangulation. The measurement area is 340 mm × 200 mm. Fig. 1b is the ricochet plate assembled on the pushcart. The structure of (c) represents the heavy metal frame to which the large witness plate is screwed (d). The witness plate has the same type of spikes at the boundaries for damping purposes. The size of the measurement area is 600 mm × 345 mm.

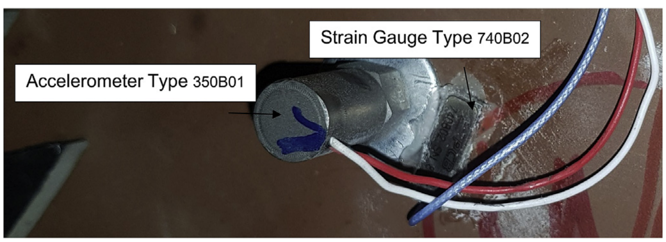

Fig. 3. Accelerometer strain gauge assembly on the witness plate.

plate is significantly larger than the ricochet plate because the spread of the second impact (from the deflected projectile or its fragments) is significantly larger compared with the first impact. The weight of the metal frame is 950 kg. This is necessary due to the strong impulse transmitted into the system during impact.

Each of the two plate types (ricochet and witness plate) is equipped with four accelerometers. The acceleration sensors are designed for severe-shock investigations up to 100,000 g 350B01 (PCB, USA) [31]. These sensors are mechanically filtered to prevent overshooting oscillations [11] and augment the capabilities to detect the incident first flexural wave. A piezoelectric strain gauge type 740B02 (PCB, USA) is also mounted on the witness plate to crosscheck the sensor signal of the accelerometer, see Fig. 3. Furthermore, the sensor plates are equipped with damping structures, which can be seen in Fig. 2a and c.

The ricochet plate has three major tasks, namely the deflection of the projectile, the position measurement, and the exact time measurement when the projectile impacts the first time. The momentum transmitted into the ricochet plate is also measured during impact, but this is not this plate's main task. The momentum measurement in the witness plate is more in focus.

Fig. 4. Thermal picture of 4 impacts with .22LR, the rise in temperature is ca. 10 °C which can easily be detected.

The witness plate's tasks are to measure the momentum and the exact point-in-time. The measurement capabilities of the witness plate need to be augmented by a thermography camera. This, because it is complex to locate different impact positions at the same time using just four accelerometers. This capability is needed because a ricochet can consist of several simultaneously impacting fragments. The thermography camera shows on the rubber screen the heat produced when a piece penetrated the thin rubber layer. The material used for the layer was a special silicone of Shore hardness 60. The layer was 0.6 mm thick. A typical picture of several impacts, which penetrated the thin rubber layer, can be seen in Fig. 4. These impacts were by subsonic projectiles weighing less than 3 g each. This penetration process showed already significant heating of the layer.

Three different ammunition types of the same calibre are investigated, as shown in Fig. 5. They have a projectile diameter of 5.56 mm, and the length of the casing is 45 mm. This calibre type was chosen to investigate the influence of the tilt angle of the ricochet plate and the different ricochet behaviour of the particular designs.

The first projectile tested is different projectile in that; it is a 5.56 mm training ammunition weighing 2.9 g. This projectile is optimised for fragmentation, see Fig. 5a. It consists of copper particles and a polymer matrix, called frangible compound. These projectile types are described less often in the scientific field. The brittle material can cause severe wounds if a person is hit by this projectile type [32,33]. For the ricochet investigation, it is an unorthodox and interesting projectile.

The second projectile type tested is the SS109, which is common and investigated extensively by tests [34] or simulation [35]. The primary reason for the development of the SS109 was to enhance the penetration capabilities of the 5.56 mm projectiles [36]. It also has a Full Metal Jacket (FMJ), but additionally features small steel core in the front of the projectile, shown in Fig. 5b. Such double-core projectiles can act differently when it comes to ricochet behaviour. The steel core can fly longer distances compared with the other projectiles. The weight of the SS109 of 4 g is the heaviest investigated.

The third ammunition type (M193) is used is a well-defined NATO standard ammunition stock number [37]. The M193 has been extensively investigated by several researchers studying terminal ballistics[38,39]. The M193 is a standard FMJ, see Fig. 5c, which makes it also a reference for ricochet measurements. The weight of the projectile is 3.6 g.

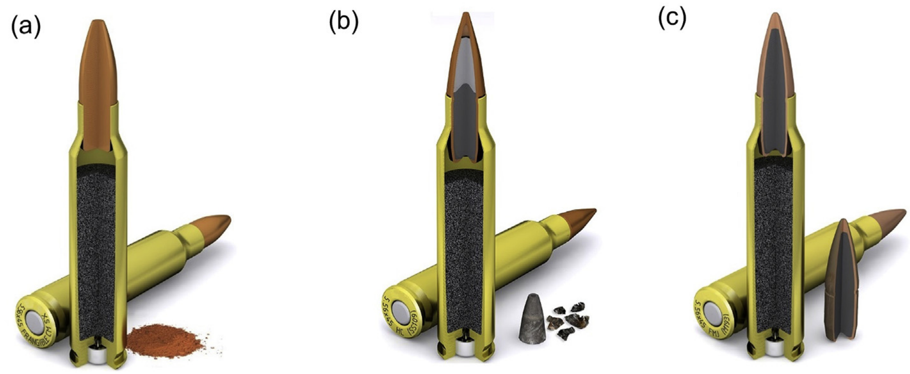

Fig. 5. Picture of the tree ammunition types investigated. Fig. 4c represents the regular FMJ projectile (M193), (b) represents the SS109 projectile with a hardened steel core. However, the basic design is still a lead core and a Metal Jacket. A different approach is described in (a). Frangible projectiles are just copper particles with a matrix, which should be transferred again to copper particles after hitting a hard target.

According to the presentation of Rottenberger [40], typical deflection angles for ricochets are 5°, 10°, 15° and 25°. Chosen for this investigation were the angles 5°, 10°, 15°, 20° and 25°. The test scope was the same as presented by the ricochet analysis of Rottenberger [40] and according to the ricochet investigations of Mattijssen and Kerkhoff [41]. Each ammunition and tilt-angle test scenario was performed five times, which means that 45 tests had to be made. The distance between the ricochet plate and the witness plate was on average 180 cm. The length was measured after every shot and noted.

The ammunition was tested with a system similar to the Electronic Pressure Velocity and Action Time (EPVAT) measurement setup [42] known for NATO tests. The National Instruments (NI, USA) USB-6366 data acquisition device was used for the tests. It can simultaneously acquire and record one set of data points every 0.5 μs The piezoelectric accelerometers are capable of measuring frequencies up to 35 kHz. The raw data with a signal amplification rate of 1 was acquired without filter, using the PCB-482C05 (PCB, USA) signal conditioner. The data acquisition time was set to 20 ms. As the signal of interest was approx. 4 ms, this acquisition time was sufficient. The pre-trigger was set to 0.1 ms. To increase the accuracy and redundancy of the measurement. The velocity was first measured ten times using a projectile light gate B471 (HPI, Austria). During the ricochet measurements, the velocity was also measured before the projectile impacts, this using a small LS260 Light Gate (Kurzzeit, Germany).

The ricochet and witness plates were calibrated with 9 mm calibration shots. A standard 9 mm projectile was accelerated to different velocities, from 290 to 350 m/s. The upper limit of the transmitted momentum was investigated using an SS109 projectile

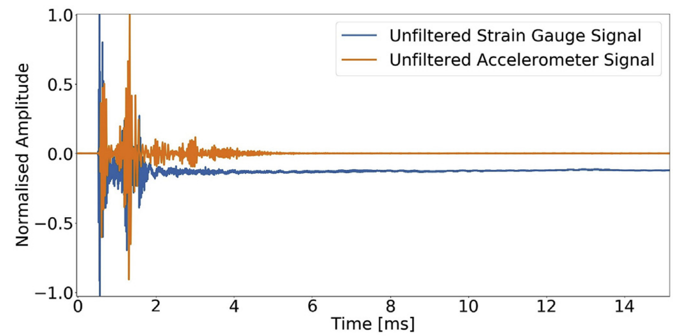

Fig. 7. Unfiltered accelerometer/strain gauge signal.

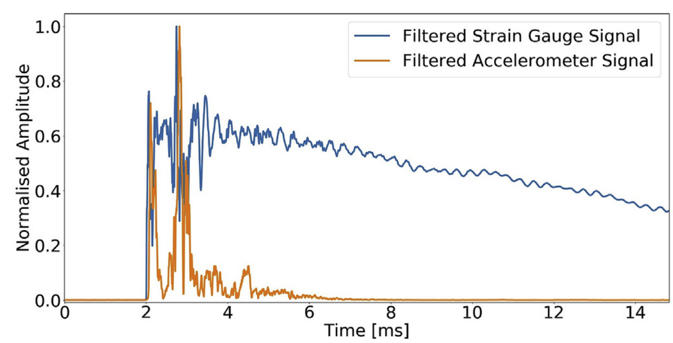

Fig. 8. Filtered accelerometer/strain gauge signal.

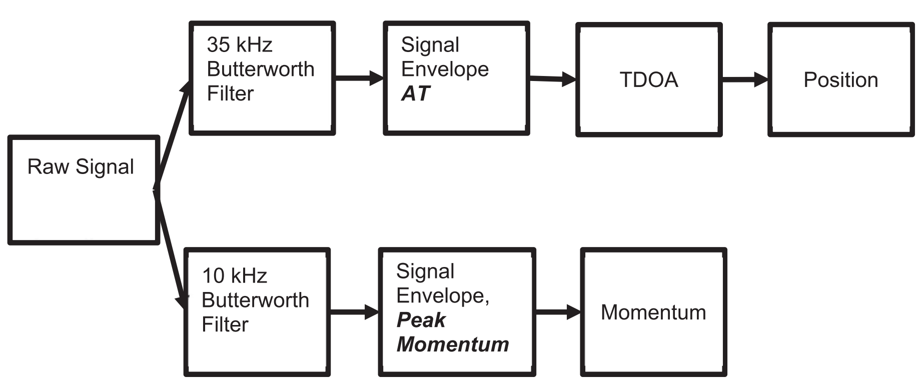

Fig. 6. Signal processing of the raw accelerometer data.

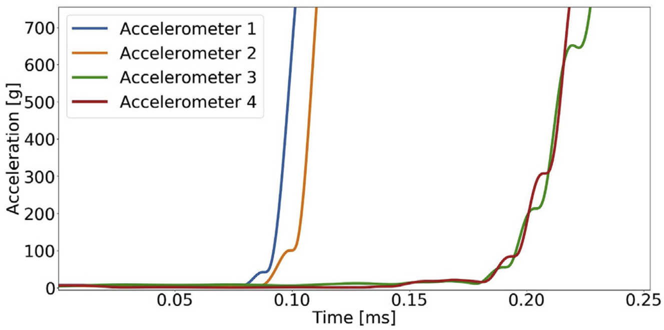

Fig. 9. Different Arrival Times of the accelerometers. This picture shows that the position of the impact was equidistant from Accelerometers 1 + 2 and 3 + 4. It also indicates that the impact is closer to accelerometers 1 and 2.

for both plate types. Both plate types were made of Hardox 500 tempered steel plate exhibiting a yield strength of 1300 MPa as a target [43]. They are regularly used for devices which are resistant to impacting supersonic projectiles [44].

This measurement was also verified by a fast-flying frangible projectile which transmitted the same momentum as the M193. All projectile types impacted orthogonal on the plates to ensure that the impact is fully inelastic. The systems can only be calibrated accurately on the assumption that the impact is inelastic. The thermal image was taken by a SeeK Compact PRO (SeeK, USA) camera. The focus of this investigation was more on the fragmentation behaviour than on the accurate triangulation. However, it was also an objective to prove that such a system can be used to enhance the positioning of impacts. The signal processing approach of this ballistic impact was the same as presented by Muster et al. [45]. An RMS envelope with low-pass filtering was applied for both detection systems, the positioning and the momentum transmitted, see Fig. 6.

3. Results

The raw data acquired from a typical accelerometer and strain gauge signal is presented in Fig. 7. The strain gauge signal rises to approximately ten μs before the accelerometer signal. This earlier rise is due to the strain gauge being slightly more sensitive than the accelerometer. However, the strain gauge shows a negative offset after being excited for 1 ms. This behaviour is even more present in the filtered case, as Fig. 8 shows. The time of the rise of the strain gauge signal is still similar to the accelerometer signal, which is important for cross-proofing purposes.

However, the strain gauge has a significantly longer recovery

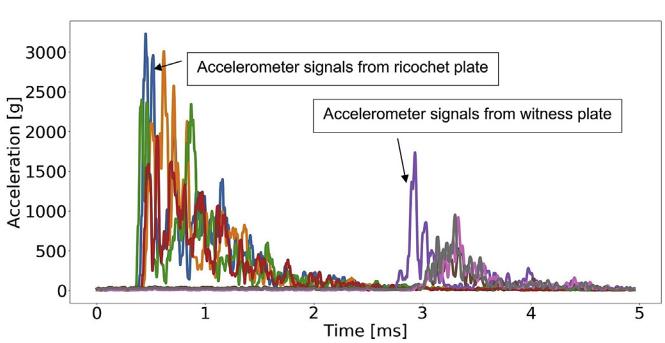

Fig. 10. Typical raw signal. The first peaks represent the acceleration signal produced on the ricochet plate. The second set of signals represents the signals of the witness plate where the ricochet impacts finally.

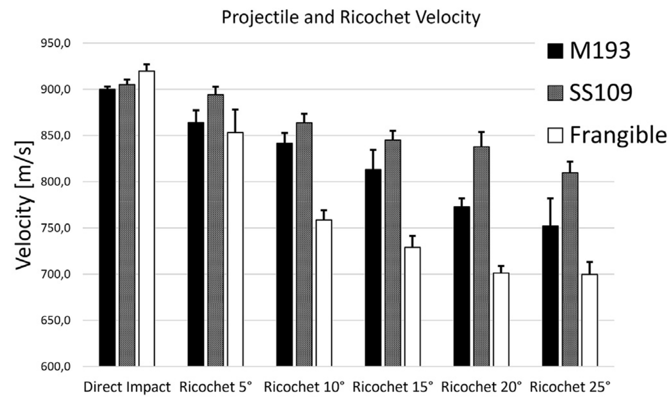

Fig. 11. Graph of the velocity the direct Impact velocity is measured using a light gate, whereas the ricochet velocities are measured using the time difference and the distance between the impact on the ricochet plate and the witness plate.

time compared to the accelerometers. This dynamic offset makes the sensor unusable for momentum detection. However, the first excitation, which is vital for the AT detection, is prominent. The AT of all four accelerometers on one plate is represented in Fig. 9. The signal rises with some small sinusoidal variations. These variations are not present in the case of the strain gauge. However, the accelerometer shows a better overall performance for the performed ballistic test scenarios.

Fig. 10 shows a typical accelerometer signal pattern of the tests. This pattern was generated by an M193 projectile under an impact angle of 15°. The first four accelerometer signals are from the ricochet plate, and they rise significantly higher compared with the second set of peaks, which come from the witness plate. This difference in maximum acceleration comes not only from the different impact strength, but also from the different stiffness's of the plates. The ricochet plate is 12 mm thick, the witness plate 30 mm. The distance between the two impacts divided by the time difference between the two sets of waves determines the ricochet velocity.

This triangulation process of the ricochet plate is more straightforward because the pre-processed acceleration signal rises strongly. The arrival time is detected by a simple threshold trigger. The acceleration pattern of the witness plate is loaded with different peaks and, just on proper AT, not visible, see Fig. 10. This pattern gives already an indication that a separation of the projectile took place, or that the projectile flies under a stronger precession and impacts diagonally. Positioning on the witness plate can be measured more accurately using a thermographic camera.

Fig. 11 shows the velocity of the impact on the witness plate. The

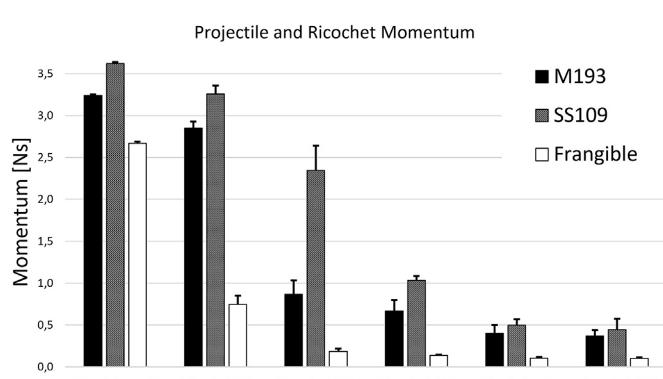

Fig. 12. Graph of the different impact momentums on the witness plate, the direct impact represents the momentum of the impact of a directly impacting projectile.

Table 1
Comparison of projectile designs.

Projectile Type	Projectile Weight [g]	Impact Angle [°]	Impact Velocity [m/s]	Ricochet Velocity [m/s]	Velocity Drop [m/s]	Momentum before Impact [Ns]	Momentum Witness Plate [Ns]	Momentum Loss before vs. after Deflection [%]
Frangible	2,9	5	920	853	67	2,67	0,75	72
Frangible	2,9	10	923	759	164	2,67	0,19	93
Frangible	2,9	15	916	729	187	2,66	0,14	95
Frangible	2,9	20	921	701	220	2,67	0,13	95
Frangible	2,9	25	917	700	217	2,66	0,10	96
M193	3,6	5	900	864	36	3,24	2,85	12
M193	3,6	10	901	841	60	3,24	0,87	73
M193	3,6	15	900	813	87	3,24	0,67	79
M193	3,6	20	900	773	127	3,24	0,41	87
M193	3,6	25	899	752	147	3,23	0,37	89
SS109	4	5	908	894	14	3,63	3,26	10
SS109	4	10	905	864	41	3,63	2,35	35
SS109	4	15	900	845	55	3,60	1,03	71
SS109	4	20	904	838	66	3,62	0,50	86
SS109	4	25	901	809	92	3,60	0,45	88

direct impact was a scenario where the projectile was shot directly at the witness plate, undeflected. It represents the normal velocity occurring 25 m after leaving the muzzle. The error bars show the standard deviation of the measured velocity. With an increasing impact angle, the velocity decreases. The velocity drop has two reasons:

Firstly, the impact wear on the steel ricochet plate. This first hit slows the projectile down, the amount of impact wear depends on the projectile material.

Secondly, the change of projectile shape. The projectile is less aerodynamic and tumbles after hitting the oblique ricochet plate.

Looking at the heavier projectiles (M193 and SS109), one can recognise a steady velocity drop. However, the slightly heavier SS109 shows a less steep linear decay than the M193. In the case of the M193, the spread of the velocity increases with an increasing ricochet plate angle. The increasing spread might be because the M193 starts to fragment and the lead fragments are of different sizes, which results in a different drag coefficient and thereby different velocities.

However, the most significant change in velocity is experienced by the frangible projectile fragments after hitting the ricochet plate. The velocity of the frangible fragments seems to plateau between 20 and 25°. This plateau effect might be because the copper powder behaves similar to a fluid after total fragmentation.

Fig. 12 shows the results of the same test scenario as in Fig. 11. This time, however, the momentum is analysed. The momentum decreases also in this case with increasing impact angle. However, with all ammunition types tested, the transmitted momentum is very low after impact on a 25° plate. Fig. 12 shows, like a fingerprint of a specific projectile design, a distinct specific momentum distribution. In the case of frangible projectiles, the momentum decays before 10° to a certain threshold below 0.1 N. In the case of the SS109, the signal decays also to a threshold. However, this threshold is reached at 20° impact. The M193 is in between in both scenarios.

The M193 shows an S-curve decay, which has its main momentum decay between 5° and 10° impact angle. Both the velocity and especially the projectile weight of the SS109 are high compared with the other ammunition types investigated, see Table 1. The momentum of the SS109 is more persistent and decays not as fast as the other projectiles. This might be due to the steel core, which behaves rigid and bounces away from the ricochet plate without substantial momentum loss.

The logarithmic decay pattern of the frangible projectile is even more present in the case of the momentum than in case of the velocity. Interestingly, the dispersion and the velocity of the 15° and 25° impacts are almost in the same range and decreased significantly compared with the initial momentum. Under these angles, the frangible projectile already fragmented into fine copper particles. These good disintegration properties are also the general purpose of frangible ammunition [46], namely the diminution of the range danger area after hitting any surface. This diminution can be quantified using the ricochet measurement device.

In Fig. 13–17, one can see the fragmentation process on a thermal picture of the investigated projectiles. The thermal image is plausible after reading the momentum graph in Fig. 12. Many impacts and a wide spread of the residuals lead to a lower overall momentum. A low total momentum is crucial for a shorter-range danger area.

Interestingly, Fig. 13 (M193) shows just one single impact, which can occur if the ricochet plate deflects the projectile more smoothly. However, this is not the case all the time; the thermal pictures

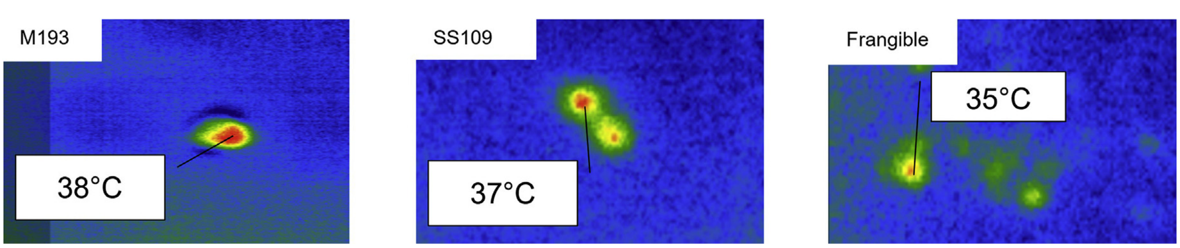

Fig. 13. Thermal impact pattern of projectiles investigated under the impact angle of 5°. The M193 does not fragmentise; the SS109 is separated into two pieces, which is a general behaviour of two cored projectiles. In the case of the frangible ammunition, one can detect already many small fragments.

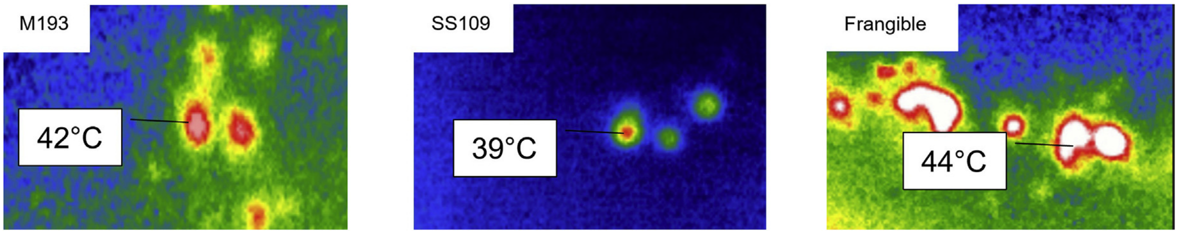

Fig. 14. Thermal impact pattern of projectiles investigated under the impact angle of 10°. The M193 fragmentise under this angle. The blurred picture of the M193 and the frangible projectile is due to temperature drifts of the thermal camera. The increase in fragmentation is recognisable primarily in the case of the frangible.

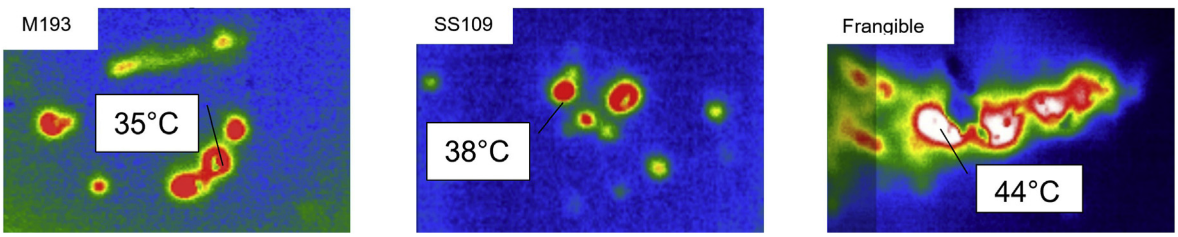

Fig. 15. Under the impact angle of 15°, all projectiles start to fragmentise. In the case of the frangible projectile, a continuous thermal pattern can be recognised. This is the impact angle, where all projectile types show a significant momentum drop.

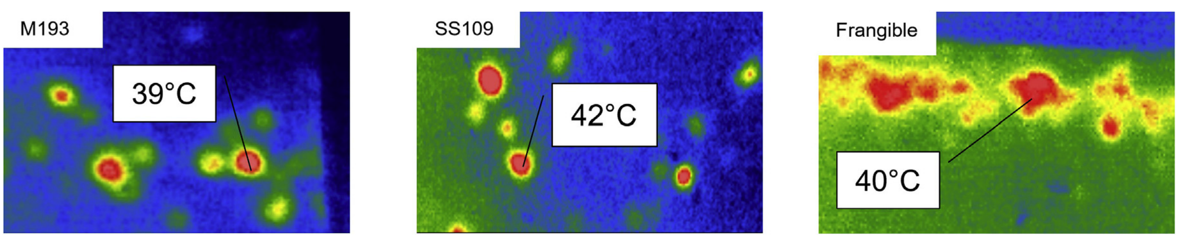

Fig. 16. Under the angle of 20°, the fragmentation spread increases for all projectiles investigated. The frangible projectile is under this angle entirely disintegrated.

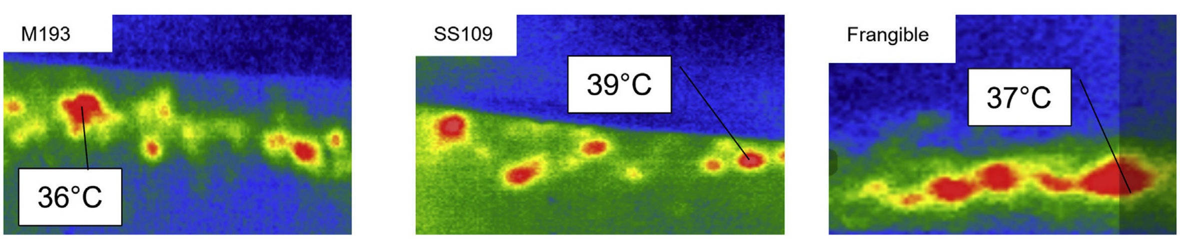

Fig. 17. Under the angle of 25°, all projectiles are entirely disintegrated and show a horizontal line pattern. This is because the projectiles are reflected under a similar angle, independent of the material and design of the projectile.

represent just a possible pattern. A problem was the temperature shift and the blurring out of the camera one can recognise this shift in the background of Figs. 13–17. Due to this fact, only the maximum temperature was indicated in the thermal images.

4. Discussion

In this ballistic experiment, positioning was performed manually by visual investigation. The results of the frangible projectile ricochets, small particles, showed that the rubber layer does not influence the test results. Even these small particles penetrate the layer easily, and the velocity is not affected by the rubber layer. In future, exact positioning with thermal imaging should be done using an algorithm-based approach.

It was not possible to conclude from the thermal signature direct to the impact strength or the shape of the ricochet. However, with a more in-depth investigation and using a camera capable of several hundred frames per second, which is more suitable for general ballistic analysis, this would be possible as part of the future work plans. Concerning the camera, there is an additional drawback that involves the temperature shift over time and the blurring of the temperature pattern, especially the background. This was the reason why only the maximal temperature was indicated. This drawback can be resolved by using a camera featuring an accurate temperature shift filter.

The momentum measurement was performed with accelerometers and a calibration step using different ammunition types. It is possible to augment the precision of the momentum measurement with precisely defined metal balls shot on the measurement plates using accurately defined acceleration machines like gas guns.

The ricochet measurement device was in this publication used to investigate 5.56 mm projectiles and 9 mm projectiles. It is also possible to use this device to investigate all small-calibre types and all different projectile types like armour-piercing projectiles with a tungsten core or solid projectiles made of brass or copper.

5. Conclusion

The goal of this work was to assess the performance and trustworthiness of a novel ricochet measurement device with ammunition types of interest. The ballistic study showed that it is possible to quantify complicated and fast-flying structures like projectiles or its ricochets with regular signal processing approaches.

A Measurement system is proposed for ballistic impact investigations, which is suitable to measure ricochet velocities and impact momentums in the typical small-calibre range.

For ballistic momentum measurements, strain gauges are less suitable than accelerometers because the signal drifts strongly in the investigated time domain. However, AT detection is possible using both strain gauges and accelerometers. For multiple impact positioning of projectile fragments, the used thermovision device is appropriate to investigate the impact pattern. However, a more precise camera with an image-processing unit would enhance the performance of this sensor approach. The momentum measured using accelerometers is a valuable property for ballistic investigations like the estimation of danger potentials of specific projectile types and their fragments.

The transmitted momentum is further connected to the range safety. A large momentum loss after a deflection on an oblique plate indicates a projectile, which has good properties for a reduced ricochet danger.

Three different ammunition types showed that the basic design of the projectiles has a significant influence on the deflection process and with this on the range danger area. The results presented here are plausible. The acquired results can be used to estimate the danger potential of the different investigated ammunition types. The investigations also confirmed that a slight deflection of regular projectile types could lead to ricochets, which are still dangerous.

The main message is that quantifying of ricochets is possible using cost-effective and straightforward devices. The concept itself can also be applied to larger or smaller calibres to support the projectile design and development process.

Acknowledgement

Special thanks go to Donald Meyer and Dr. Peter Spatz who made these measurements possible. The authors would like to thank RUAG Ammotec AG Switzerland for the provision of the test facilities and equipment. The use of measurement devices would not have been possible without the great help of Markus Gruenig and Roland Niederhaeuser.

References

[1] Kusano H, Aoki Y, Hirano Y, Kondo Y, Nagao Y. High-speed imaging on static tensile test for unidirectional CFRP. Proc *SPIE* 2009;7126.
[2] Chou P, Toland R. Experimental study of multiple interior impacts. 1976. p. 201−2.
[3] Yan XL, et al. Characterization of a double Time-Of-Flight detector system for accurate velocity measurement in a storage ring using laser beams. Nucl Instruments Methods Phys Res Sect A Accel Spectrometers, Detect Assoc Equip 2019;931(March):52−9.
[4] Courtney M. Acoustic methods for measuring bullet velocity. Appl Acoust 2008;69:925−8.
[5] Espinosa HD. Low-velocity impact testing, vol. 8; 2000. p. 539−59.
[6] Espinosa HD, Raiser G, Clifton RJ, Ortiz M. Performance of the star-shaped flyer in the study of brittle materials: three dimensional computer simulations and experimental observations. J Appl Phys 1992;72(8):3451−7.
[7] Morsy R, Marzouk H, Haddara M, Gu X. Multi-channel random decrement smart sensing system for concrete bridge girders damage location identification. Eng Struct 2017;143:469−76.
[8] Dahlen U, Ryden N, Jakobsson A. Damage identification in concrete using impact non-linear reverberation spectroscopy. NDT E Int 2015;75:15−25.
[9] Allaeys F, Luyckx G, Van Paepegem W, Degrieck J. Development and validation of a set-up to measure the transferred multi-axial impact momentum of a bird strike on a booster vane. Int J Impact Eng 2017;99:102−10.
[10] Hammetter CI, Jones RL, Stauffacher HL, Schoenherr TF. Measurement and modeling of supersonic hailstone impacts. Int J Impact Eng 2017;99:48−57.
[11] Agnello A, Dosch J, Metz R, Sill R, Walter P. Acceleration sensing technologies for severe mechanical shock. Sound Vib 2014;48(2):8−U20.
[12] T H, O C, G D, C J, S R, Touzé C. Wave turbulence in vibrating plates: the effect of damping. EPL (Europhys Lett) 2013;102(3):30002.
[13] Zhao G, Hu H, Li S, Liu L, Li K. Localization of impact on composite plates based on integrated wavelet transform and hybrid minimization algorithm. Compos Struct 2;176:234−43.
[14] Perelli A, De Marchi L, Marzani A, Speciale N. Frequency warped cross-wavelet multiresolution analysis of guided waves for impact localization. Signal Process 2014;96(PART A):51−62.
[15] Mušicki D, Kaune R, Koch W. Mobile emitter geolocation and tracking using TDOA and FDOA measurements. IEEE Trans Signal Process 2010;58(3 PART 2): 1863−74.
[16] Gustafsson F, Gunnarsson F. Positioning using time-difference of arrival measurements. In: IEEE international conference on acoustics, speech, and signal processing, vol. 6; 2003. p. 553−6. vol. 6.
[17] Liu M, Yang J, Cao Y, Fu W, Cao Y. A new method for arrival time determination of impact signal based on HHT and AIC. Mech Syst Signal Process 2017;86(April 2016):177−87.
[18] Krylov VV, Tilman FJBS. "Acoustic 'black holes' for flexural waves as effective vibration dampers. J Sound Vib 2004;274(3−5):605−19.
[19] Krylov VV, Winward RETB. Experimental investigation of the acoustic black hole effect for flexural waves in tapered plates. J Sound Vib 2007;300(1−2): 43−9.
[20] Bowyer E, Krylov V. Acoustic black hole manufacturing for practical applications and the effect of geometrical and material imperfections. 2016. p. 2411−21. no. 4.
[21] Howard A. Morphological control of censile release in ceramic penetration. Cranfield University; 2014.
[22] Muster M, Hameed A, Wood D, Appleby-Thomas G, Wasmer K. Damping of post-impact vibrations. Appl Acoust 2019;156:427−33.
[23] Manrad P. SYSTEMAND method for calculating ROJECTILE impact COORONATES. 2008.
[24] Johnston JP, Pereira JM, Ruggeri CR, Roberts GD. High-speed infrared thermal imaging during ballistic impact of triaxially braided composites. J Compos Mater 2018;52(25):3549−62.
[25] Domun N, et al. Ballistic impact behaviour of glass fibre reinforced polymer composite with 1D/2D nanomodified epoxy matrices. Compos B Eng 2019;167:497−506.
[26] Swiderski W, Hlosta P. Non-destructive evaluation of impacted CFRP by IR thermography. Materials 2019;12(6):956.
[27] Gopalakrishnan S, Senthil V. Failure analysis of ballistic material. Int Conf Adv Mater Eng 2011;15:95−100.
[28] Duan Y, et al. Reliability assessment of pulsed thermography and ultrasonic testing for impact damage of CFRP panels. NDT E Int 2019;102:77−83.
[29] Hwang S, An YK, Sohn H. Continuous line laser thermography for damage imaging of rotating wind turbine blades. Procedia Eng 2017;188:225−32.
[30] Spiridonakos MD, Fassois SD. Vibration based fault detection in a time-varying link structure via non-stationary FS-VTAR models. In: Proceedings of the International Operational Modal Analysis Conference (IOMAC), Ancona, Italy; 2009. p. 315−22.
[31] PCB, High shock ICP ® accelerometer.
[32] Komenda J, et al. Forensic and clinical issues in the use of frangible projectile. J Forensic Leg Med 2013;20(6):697−702.
[33] Martrille L, Artuso A, Cattaneo C, Baccino E. A deceptive case of gunshot entry wounds - beware of frangible bullets. J Forensic Leg Med 2007;14(3):161−4.
[34] Horsfall I, Crewther IR. Proc 19th international symposium on ballistics. In: Glass ceramic armour systems for light armour applications; 2001.
[35] Vanichayangkuranont T, Maneeratana K, Chollacoop N. Numerical Simulations of level 3A ballistic impact on ceramic/steel armor. 2006. p. 2−7. no. October.
[36] Arvidsson PG. Is there a problem with the lethality of the 5.56 NATO caliber. 2009.
[37] States U, Arms R. 5.56×45mm NATO. 1963.
[38] Ragsdale B, Sohn S. Comparison of the terminal ballistics of Full metal Jacket 7.62-mm M80 (NATO) and 5.56-mm M193 military bullets: a study in ornance gelatin BT. 1988.
[39] Sturtevant B. Shock wave effects in biomechanics. Sadhana 1998;23(5): 579−96.
[40] Rottenberger I. Abprallverhalten von Jagdmunition. 2011. p. 105.
[41] Mattijssen EJAT, Kerkhoff W. Bullet trajectory reconstruction - methods, accuracy and precision. Forensic Sci Int 2016;262:204−11.
[42] AEP-97, *Multi calibre manual of proof and inspection (M-C MOPI) for 5.56 mm, 7.62 mm, 9 mm and 12.7 mm ammunition*, vol. vol. 23, no. December 2013.

2014.
[43] Dudziński W, Konat Ł, Pękalski G. Structural and strength characteristics of wear-resistant martensitic steels. Arch Foundry Eng 2008;8(2):21–6.
[44] Hub J, Komenda J. Ballistic resistance of steel plate hardox upon impact of non-penetrating projectiles. Adv Mil Technol 2009;4(2):79–91.
[45] Muster M, Hameed A, Wood D. Dynamic qualitative bolt force measurements for investigating influence factors on the pushout effect of small calibre ammunition. AIP Adv 2019;9(6):065020.
[46] Mates SP, Rhorer R, Banovic S, Whitenton E, Fields R. Tensile strength measurements of frangible bullets using the diametral compression test. Int J Impact Eng 2008;35(6):511–20.